Southern African Large Telescope

PFIS Distortion and Alignment Model

Kenneth Nordsieck
University of Wisconsin

Document Number: SALT-3120AS0023

Revision 2.0
31 May 2006

Change History

Rev	Date	Description
1.0	2 Mar, 2005	Original
2.0	31 May, 2006	Added flexure section

Table of Contents

1 Scope

This document describes the mathematical model that is used to correct for the PFIS CCD mosaic alignment, detector dewar alignment, mechanical flexure, and optics distortion as a function of configuration, wavelength and temperature. The SALT IRAF package maintains two files, PFISgeom.dat and PFISdistortion.dat, containing the relevant parameters.

2 Alignment

The following static alignment parameters were determined in PFIS imaging mode using a Cartesian grid slitmask with pinholes every 5 mm. Alignment parameter entries in the IRAF data files are dated, since they may change as the result of detector alignment or dewar servicing.

2.1 CCD Mosaicing

The PFIS detector consists of three EEV 2048x4096 CCD's, mosaiced with a gap of 90 - 100 unbinned pixels. The alignment of chips 1 and 3 were defined relative to chip 2 as follows: $\Delta\phi$ is the rotation, and Δx and Δy is the offset of the center of the chip from where it would be if the rotation were zero with zero gap.

Chip	$\Delta\phi$ (deg)	Δx (pix)	Δy (pix)
1	0.0735	-104.56	3.24
3	-0.0380	91.87	1.31

Table 1. CCD chip mosaic

These parameters are kept in PFISgeom.dat, and are used to mosaic the multi-extension file into a single FITS file. These were determined from a distortion calibration taken at 630 nm on 1 Dec 2004. A comparison with the subsequent calibration on 24 Feb, 2005, reveals an error of roughly 0.5 pixels in Δx and Δy, and 0.04 deg in $\Delta\phi$. Since these were determined using different masks, and the mask error is about 0.3 pixels, this error may be mostly in the mask. A better calibration awaits a sky image.

2.2 Detector Alignment

The detector alignment is defined by three parameters, ϕ, x_0, and y_0, which are the rotation of the central chip with respect to the instrument coordinate system, and the unbinned pixel coordinates of the optical axis (defined by the Cartesian pinhole mask). Relative to the "central" pixel of the center CCD ($x_c = 1024$, $y_c = 2048$), the current alignment is,

$$\phi = -0.1226 \text{ deg}$$

$$x_0 - x_c = -0.749 \text{ pixels}$$

$$y_0 - y_c = 13.776 \text{ pixels}$$

These were determined from the mean of distortion calibrations in five interference filters on 24 Feb, 2005. The RMS error among the five determinations was ±0.23 pixels for x and y, and

0.0006 deg (2.2 arcsec) in rotation. There is a systematic shift in y of about 0.5 pixel from 400 to 800 nm.

3 Flexure

A model of image motion due to flexure of the PFIS structure and optomechanical mounts has been constructed using data taken on the telescope using the pinhole and cartesian grid slitmasks, as a function of rho stage position and of tracker tip/ tilt. This has been compared with the post-CDR FEA model.

3.1 Imaging Mode

In imaging mode the positions of slitmask holes at the center, left, right, top, and bottom of the 8 arcmin field were measured, for three sequences of tracker positions, defined by the standard tracker coordinate system ρ, θ, and ϕ. For tracker tip-tilt, a spherical polar coordinate system with pole at the tracker-centered position was defined as follows: α = polar angle, β = azimuthal angle = $\tan^{-1}(\phi/\theta)$.

- θ = ϕ = 0 (tracker centered), ρ = -100, -80 ... 80, 100°
- ρ = 0, α = 6°, β = 0, 30 .. 330°
- ρ = 90°, α = 6°, β = 0, 30 .. 330°

Figure 1 displays the ρ variation. The left two panels show the image motion in the *x* and *y* directions, for the center, and for the left and right (*y*) and top and bottom (*x*) pinholes. The difference between the center and edge pinholes is due entirely to flexure-induced image rotation. This image rotation is shown in the upper right panel. The lower right panel shows the track of a pixel in *x* and *y* as a function of ρ. The thick line shows the results of the CDR FEA model, updated to account for the expected ρ-stage flexibility. There are two major effects which cause the image motion to be more than expected: 1) there is an unmodeled effect which makes

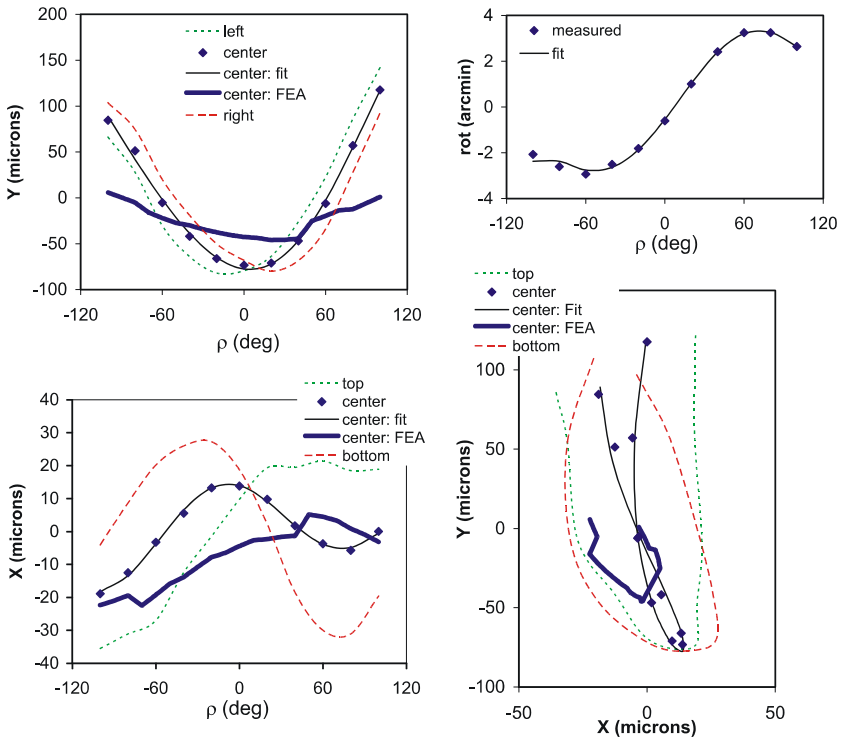

Figure 1. Imaging mode flexure vs ρ stage angle

the y flexure about 3× expected, and 2) image rotation was not modeled, which contributes in x for the top and bottom of the field of view. Except for the rotation effect, the x motion is comparable to the FEA model. The thin lines show a simple two-harmonic sinusoidal fit to the x, y, and rotation image motion, as given by the following formulae

$$\delta f(\rho) = A_1 \cos(\rho + P_1)$$

$$+ A_2 \cos(2\rho + P_2).$$

Figures 2 and 3 display the β-variation, with the tracker at maximum deflection (α = 6°), for two different ρ-stage positions. The y image motion is again about 2.5 times expected, while the x motion agrees rather well with the FEA model. The motion due to tracker tip/ tilt can be can be well modeled with a single harmonic, assuming that the ρ- and α- dependent flexures are independent, and the α- flexure is linear with α:

$$\delta f(\beta) = A_3 (\alpha/6°)$$

$$\times\cos(\beta + \rho + P_3).$$

Table 2 gives the best-fit coefficients. The combined tip/tilt and rotation fit is accurate to roughly 5 μ.

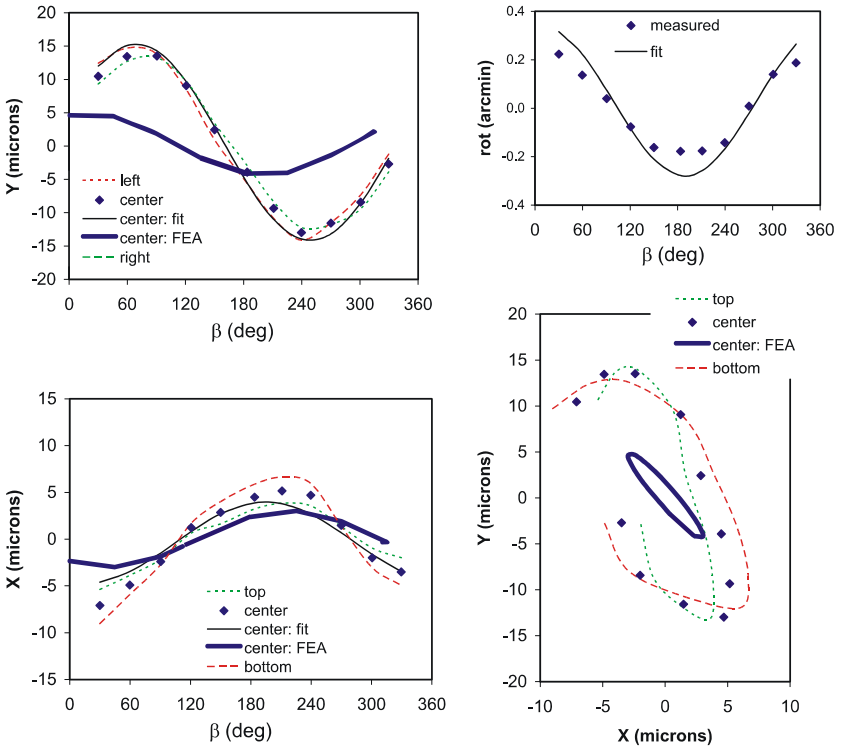

Figure 2. Tip/Tilt image motion at ρ=0°.

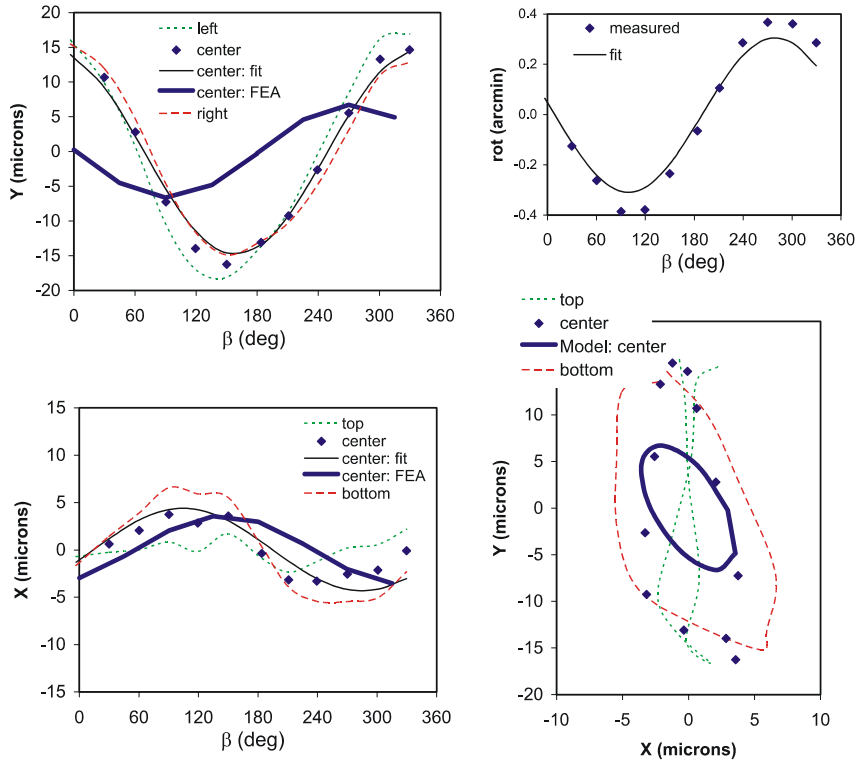

Figure 3. Tip/Tilt image motion at ρ=90°

Variable	A_1	P_1 (°)	A_2	P_2 (°)	A_3	P_3 (°)
x (μm)	-7.41	119.1	12.18	33.5	4.35	-194.5
y (μm)	-157.57	3.8	-10.95	-101.9	-14.72	110.9
rotation (‘)	3.54	-34.6	1.51	-114.8	0.31	-9.2

Table 2. Flexure Model Coefficients

With this flexure model, we can predict the total flexure in imaging mode over a SALT track. Figure 4 shows the worst case flexure (using the most unfavorable starting ρ position) for different declination tracks using the full ±6° tracker motion. Note that the values are double valued because the roll-dependent and tip/tilt-dependent image motion do not sum the same way on the East and West sides of the SALT observing annulus. In general, the worst-case motion in the dispersion direction is comparable to the specification, except for targets at the bottom of the field of view in the South. Worst-case motion perpendicular to the dispersion direction reaches 6× the specification at the most Southerly declinations. The additional y motion can be assigned to two different sources, underestimated ρ-stage fixed or load-dependent bending, or flexure of an internal PFIS optical element that was not correctly modeled. We believe the test results implicate the latter. A ρ-stage flatness problem would show up only in the rotation-dependent image motion, since during rotation the structure is warped as the interface pads cross the supporting hexapod legs. The tip/tilt dependence would not be affected by ρ-stage flexure, since the ρ-stage-imposed flexure would be constant. Since both the rotation and tip/tilt data exhibit a 2-3× increased flexure which matches the FEA model poorly, the problem must be internal to PFIS, and it must affect y-motion only. The fold mirror or the collimator doublet seem to be the likely culprits. The ρ-stage is in fact probably stiffer than was used in the FEA analysis: ρ-stage flexibility shows up as a 3ρ harmonic, due to the 3-fold symmetry of the hexapod legs. The third harmonic is seen to be much weaker in the data (see figure 1) than in the FEA model.

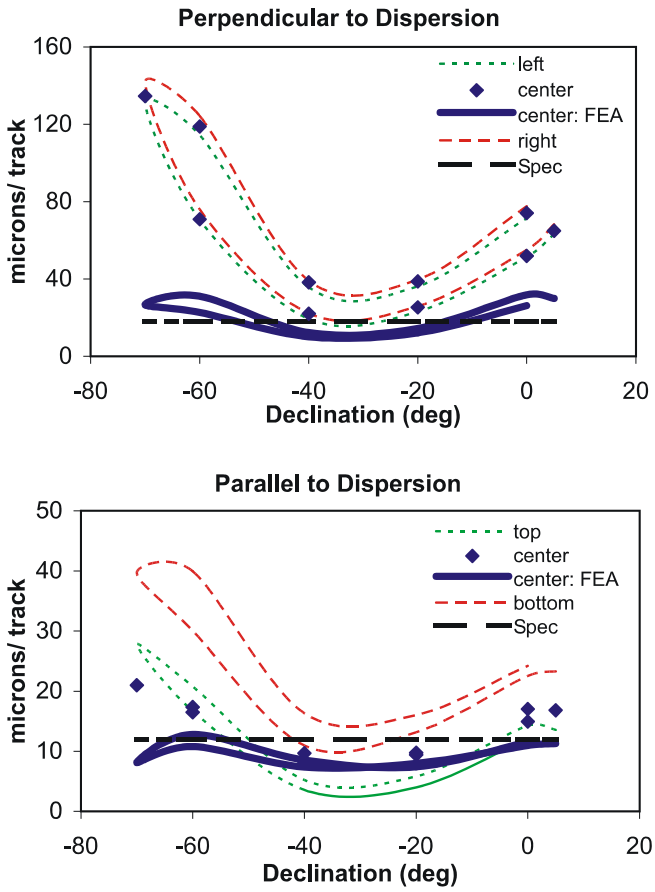

Figure 4. Worst-case PFIS image motion over a SALT track (imaging mode)

3.2 Spectroscopic Mode

TBS

4 Distortion

A model of the optical distortion between the slitmask plane and the detector plane was constructed using the PFIS ZEMAX raytracing model. In imaging mode, it is a function of field angle, wavelength, and temperature (in order of decreasing sensitivity). In spectroscopic mode, there is an additional distortion due to spectral line curvature and due to the change in anamorphic magnification in the direction of dispersion. The distortion model has so far been verified in imaging mode at five wavelengths and one temperature.

4.1 Imaging Mode

Imaging mode distortion is defined by a function of three parameters, R_{max}, A , and B , where A and B are cubic and fifth order distortion coefficients, and R_{max} gives the undistorted "normalized pixel scale" in mm/ 4 arcmin. All are normalized at ρ_{max} = 4 arcmin, the maximum field angle. The distance R in mm from the optical axis at the detector is then given by:

$$R/R_{max} = (r/r_{max}) + A\,(r/r_{max})^3 + B\,(r/r_{max})^5$$

where r is the distance from the optical axis and r_{max} is the normalized pixel scale at the slitmask plane. (We currently assume zero telescope distortion, and with r_{max} = (240 arcsec/1000)×223.8 microns/arcsec = 53.712 mm).

The PFIS chromatic lateral aberration makes R_{max}, and to a lesser extent, A and B, a function of wavelength. This dependence has been modeled empirically as follows

$$R_{max}(\lambda) = R_0 + R_1\,\lambda + R_2 / \lambda^2 + R_3 / \lambda^3$$

$$A(\lambda) = A_0 + A_1 / \lambda + A_2 / \lambda^2$$

$$B(\lambda) = B_0 + B_1 / \lambda + B_2 / \lambda^2$$

Finally, R_{max}, A, and B are weak functions of temperature, which may be modeled empirically by treating their wavelength coefficients $f_{0,1,2,3}$ as functions f(T)

$$f(T) = f + f_t\,(T_h - T) / (T_h - T_c)$$

where T_c = -5° C and T_h = 20° C, the operational temperature limits of the spectrograph. This is formulated so that the coefficients with *0 - 3* subscripts all apply at T = T_h = 20°C, and the coefficients with additional *t* subscripts give the corrections to these. These coefficients have been evaluated by fitting the distortion coefficients from raytraces at 7 wavelengths and the two extreme temperatures. In Table 3 the coefficients are given assuming wavelengths in microns.

Subscript	R_{max} (mm)	$R_{max,\,t}$	A	A_t	B	B_t
0	27.6485	0.0165	0.013283	0.000104	0.008488	0.000095
1	0.4246		0.000296	-0.000010	-0.000716	-0.000024
2	0.0620	-0.0012	-0.000273		0.000167	
3	-0.0150					

Table 3. PFIS Distortion Model Coefficients

Figures 5 and 6 illustrate the distortion coefficients derived from the raytracings (symbols), and their fits to wavelength and temperature (+20C: line; -5C: dashed). Open symbols represent coefficients derived from the 24 Feb, 2005 distortion calibrations. The latter assumes a B coefficient taken from the raytrace. The fit with B allowed to vary gives a B within about 5% of the raytrace, with errors at least that large. The wavelength and temperature coefficients will be adjusted as more data comes in.

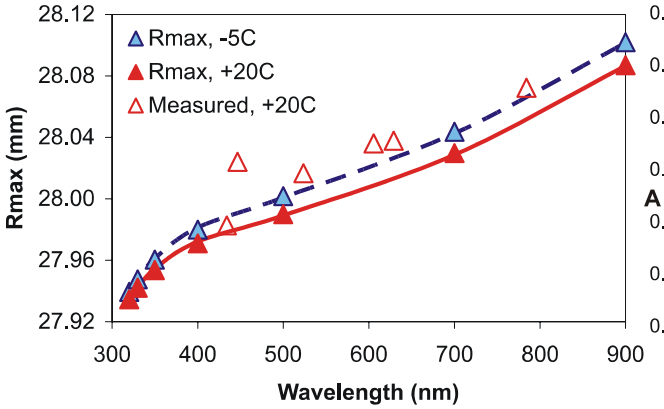

Figure 5. Focal plane scale vs wavelength

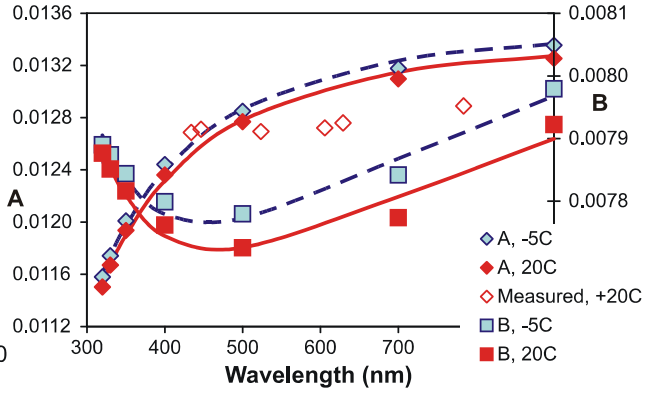

Figure 6. Distortion Coefficients

4.2 Spectroscopic Mode

In grating spectroscopy, there are two further corrections to the imaging mode distortion, spectral line curvature, and differential anamorphic magnification. We first make the approximation that the imaging distortion occurs before the grating, which is a good approximation for PFIS, for which the collimator distortion is an order of magnitude large than the camera distortion. Next, we assume that the grating and camera articulation angles are near Littrow ($\beta \cong \alpha$, where α = incidence angle and β = diffraction angle). It can then be shown, by expanding the grating equation for small out-of-plane angles and small off-Littrow angles, the curvature correction $\delta x'_c$ at the detector in the dispersion direction as a function of the cross-dispersion position y is

$$\delta x'_c (x',y) \cong (y^2 / f) \tan \alpha \ (1 - x' \tan \alpha \ / f)$$

where α is the grating incidence angle on-axis, f is the focal length of the camera (330 mm), and x' is the x-position relative to the on-axis Littrow wavelength position x_L . For operation near Littrow (central diffraction angle $\beta_0 \cong \alpha$), x_L may be approximated by

$$x_L \cong x_0 + (\beta_0 - \alpha) f$$

Finally, a correction must be made for the change in anamorphic magnification $\cos(\alpha)/\cos(\beta)$ in the direction of dispersion. Again expanding around the Littrow wavelength which falls at x_L, we should find for the anamorphic magnification correction $\delta x'_a$

$$\delta x'_a (x') \cong (x'^2 / f) \tan \alpha (1 + x' \tan \alpha / f)$$

(Actually, all my attempted derivations give a 4/3 coefficient of the last tan α, oh well! The above seems to fit much better)

Applying the first term of the curvature correction to the magnification correction, and summing, we obtain for the total correction,

$$\delta x'(x',y) \cong (r'^2 / f) \tan \alpha + (x' r'^2 / f^2) \tan^2 \alpha$$

where $r'^2 = x'^2 + y^2$.